DTU Library

Experimental demonstration of intermodal nonlinear effects between full vectorial modes in a few moded fiber

Rishøj, Lars Søgaard; Kristensen, Poul; Ramachandran, Siddharth; Rottwitt, Karsten

Published in:
Optics Express

Link to article, DOI:
10.1364/OE.21.028836

Publication date:
2013

Document Version
Publisher's PDF, also known as Version of record

Experimental demonstration of intermodal nonlinear effects between full vectorial modes in a few moded fiber

Lars Rishøj,[1,*] **Poul Kristensen,**[2] **Siddharth Ramachandran,**[3] **and Karsten Rottwitt**[1]

[1]*Technical University of Denmark, Ørsteds plads 343, 2800 Kgs. Lyngby, Denmark*
[2]*OFS-Fitel, Priorparken 680, 2605 Brøndby, Denmark*
[3]*Boston University, 8 Saint Mary's Street, Boston, MA 02215, USA*

[*]*lris@fotonik.dtu.dk*

Abstract: We experimentally investigate intermodal nonlinear interactions, such as Raman scattering and four wave mixing. The fiber used is a specially designed few moded fiber, which splits the degeneracy of the first mode group, leading to stable propagation of the two full vectorial modes, TM_{01} and TE_{01}. For the Raman experiments pumping occur in either the fundamental mode or the two full vectorial modes, whereas the signal is in the fundamental mode. In all three experiments approximately 40 dB of gain is achieved using 307 W of pump peak power. When pumping in either of the full vectorial modes four wave mixing is observed.

OCIS codes: (190.4370) Nonlinear optics, fibers; (190.5650) Raman effect; (190.4223) Nonlinear wave mixing.

References and links

1. M. Ziemienczuk, A. M. Walser, A. Abdolvand, and P. S. J. Russell, "Intermodal stimulated Raman scattering in hydrogen-filled hollow-core photonic crystal fiber," J. Opt. Soc. Am. B **29**, 1563–1568 (2012).
2. B. M. Trabold, A. Abdolvand, T. G. Euser, A. M. Walser, and P. S. Russell, "Amplification of higher-order modes by stimulated Raman scattering in h_2-filled hollow-core photonic crystal fiber," Opt. Lett. **38**, 600–602 (2013).
3. K. Rottwitt and J. Povlsen, "Analyzing the fundamental properties of Raman amplification in optical fibers," J. Lightwave Technol. **23**, 3597–3605 (2005).
4. C. Antonelli, A. Mecozzi, and M. Shtaif, "Raman amplification in multimode fibers with random mode coupling," Opt. Lett. **38**, 1188–1190 (2013).
5. R. Ryf, A. Sierra, R.-J. Essiambre, S. Randel, A. Gnauck, C. A. Bolle, M. Esmaeelpour, P. J. Winzer, R. Delbue, P. Pupalaikis, A. Sureka, D. Peckham, A. McCurdy, and R. Lingle, "Mode-equalized distributed raman amplification in 137-km few-mode fiber," in "European Conference and Exposition on Optical Communications," p. Th.13.K.5 (2011).
6. R. H. Stolen, "Phase-matched-stimulated four-photon mixing in silica-fiber waveguides," IEEE J. Quant. Electron. **11**, 100–103 (1975).
7. L. Rishj, P. Steinvurzel, Y. Chen, L. Yan, J. Demas, M. Grogan, T. Ellenbogen, K. Crozier, K. Rottwitt, and S. Ramachandran, "High-energy four-wave mixing, with large-mode-area higher-order modes in optical fibres," in "European Conference and Exposition on Optical Communications," p. Tu.3.F.2 (2012).
8. J. Ramsay, S. Dupont, M. Johansen, L. Rishøj, K. Rottwitt, P. M. Moselund, and S. R. Keiding, "Generation of infrared supercontinuum radiation: spatial mode dispersion and higher-order mode propagation in ZBLAN step-index fibers," Opt. Express **21**, 10764–10771 (2013).
9. F. Poletti and P. Horak, "Dynamics of femtosecond supercontinuum generation in multimode fibers," Opt. Express **17**, 6134–6147 (2009).
10. S. Ramachandran, P. Kristensen, and M. F. Yan, "Generation and propagation of radially polarized beams in optical fibers," Opt. Lett. **34**, 2525–2527 (2009).

#197744 - $15.00 USD Received 17 Sep 2013; revised 10 Oct 2013; accepted 11 Oct 2013; published 15 Nov 2013

11. S. Ramachandran, C. Smith, P. Kristensen, and P. Balling, “Nonlinear generation of broadband polarisation vortices,” Opt. Express **18**, 23212–23217 (2010).
12. R. H. Stolen, “Polarization effects in fiber Raman and Brillouin lasers,” IEEE J. Quant. Electron. **15**, 1157–1160 (1979).
13. J. Bromage, K. Rottwitt, and M. Lines, “A method to predict the Raman gain spectra of germanosilicate fibers with arbitrary index profiles,” IEEE Photon. Technol. Lett. **14**, 24 –26 (2002).
14. J. Hansryd, P. Andrekson, M. Westlund, J. Li, and P.-O. Hedekvist, “Fiber-based optical parametric amplifiers and their applications,” IEEE J. Sel. Topics Quantum Electron. **8**, 506–520 (2002).

1. Introduction

In the past years intermodal Raman scattering has received increasing attention. For example, interaction between linearly polarized psedomodes in a hollow-core photonic crystal fiber (PCF) was studied in [1, 2]. Also from a theoretical point of view the implications of having a pump in multiple modes was investigated in [3], and Raman amplification in multimode fibers in the presence of random mode coupling within degenerated mode groups was presented in [4]. An important application for intermodal Raman scattering is amplifiers for spatial division multiplexing (SDM) systems using few-moded fibers (FMFs), which are proposed as a means to expand the optical communication bandwidth. Especially for long-haul communication optical amplification is crucial, in this regard FMFs have the advantage of intensity overlap between the different modes, which enables sharing of a single pump between multiple signal modes [5]. Another phenomenon observed in this paper is four wave mixing (FWM) between higher order modes (HOMs). This was first experimentally demonstrated decades ago [6], and more recently it was utilized for modulation instability in the 1 μm-regime in a large area mode (A_{eff} = 618 μm^2) [7]. An application where both intermodal Raman and FWM interactions are relevant is supercontinuum generation, since the presence of HOMs is known to have a profound impact on the generated spectrum [8, 9].

In this paper, measurements on intermodal nonlinear mixing are presented for a specialty designed fiber [10]. The pump is either in the fundamental mode, HE_{11}, or one of the two full vectorial modes, TM_{01} or TE_{01}, whereas the signal is always in the HE_{11} mode. Previously, spontaneous Raman scattering was demonstrated in the fiber used in this paper to generate vortex beams over a broad wavelength range by pumping at 1064 nm [11].

2. Experimental setup

The refractive index profile of the FMF used in the experiments is shown in Fig. 1. The fiber

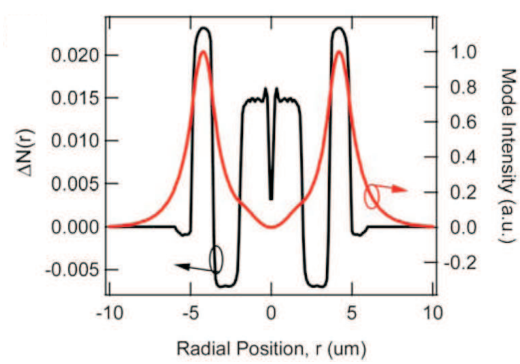

Fig. 1. Refractive index profile (black) similar to FMF, and the radial intensity profile for the TE_{01} mode (red) [10].

#197744 - $15.00 USD Received 17 Sep 2013; revised 10 Oct 2013; accepted 11 Oct 2013; published 15 Nov 2013

design eliminates the degeneracy of the first mode group consisting of the TM_{01} mode (radially polarized), the TE_{01} mode (azimuthally polarized), and the two degenerated modes HE_{21} (mixed polarized). Therefore, strong mode coupling within the first mode group yielding the familiar LP_{11} modes is avoided, and controlled excitation of the individual full vectorial modes is ensured, together with stable propagation along the fiber. This fiber was first presented in [10].

The schematic of the experimental setup is provided in Fig. 2. The pump source is a Q-

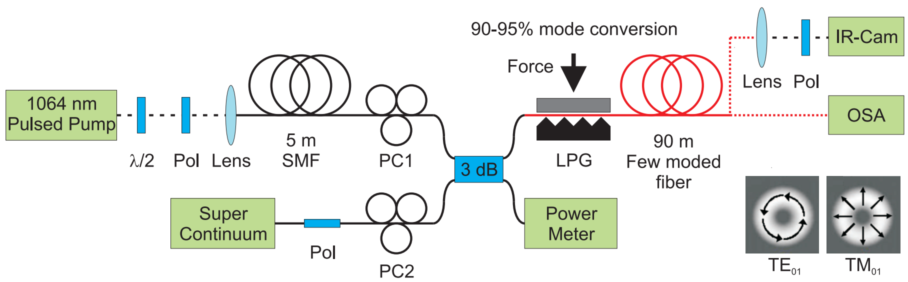

Fig. 2. Schematic of the experimental setup.

swithed Nd:YAG laser producing 700 ps pulses, with a peak power of 21 kW, and a repetition rate of 6 kHz. The pump laser is coupled into 5 m of single moded fiber (SMF), in which the seed signal is generated via spontaneous Raman scattering. The mode excitation of the pump is performed in the few moded fiber (FMF) using a long period microbend grating (LPG). The grating is created by pressing an aluminum block with periodic grooves and a rubber pad together. Insets are provided of the two modes of interest; the arrows indicate the polarization of the mode. A supercontinuum source is used when tuning the resonance wavelength of the grating; this is done by rotating the grating block. The mode coupling is maximized by adjusting the polarization controller (PC1) and the pressure applied to the rubber pad, responsible for creating the grating. Typical conversion efficiencies between the fundamental mode and either of the HOMs are approximately 95 %. The output of the FMF is either measured with an OSA or imaged on a camera. In the experiments the pump is either in the HE_{11}, TM_{01}, or TE_{01} mode. The signal generated via Raman scattering, in the initial 5 m of SMF, remains in the HE_{11} mode in the FMF, which is ensured since the splice from SMF to FMF was optimized to minimize mode coupling, and also the LPG does not excite HOMs at the wavelength region of the first order Raman peak.

3. Nonlinear interactions

The spectra shown in Fig. 3 are the average power after both 1 m (immediately after the LPG) and 90 m of propagation in the FMF. The pump is in either HE_{11}, TM_{01}, or TE_{01} mode as indicated by the legend, whereas the signal is in the fundamental mode. Based on average power measurements, the launched peak power is estimated to be 307 W. It is noted that the saturation level of the OSA is at -20 dBm, so saturation is reached at the wavelength of the pump. The net gain through the FMF, defined as $P_{\mathrm{L=90m}}/P_{\mathrm{L=1m}}$, is approximately 40 dB for all three pump modes.

The strength of the Raman scattering process depends primarily on the co-polarized intensity overlap integral between the interacting modes. However, even though this overlap integral is smaller when the pump is in the TM_{01} and TE_{01} modes, these modes have the unique feature of being inherently polarization preserving [10]. Hence, theoretically the strength of Raman scattering becomes independent of polarization walk-off, which is known to reduce the gain by

#197744 - $15.00 USD Received 17 Sep 2013; revised 10 Oct 2013; accepted 11 Oct 2013; published 15 Nov 2013

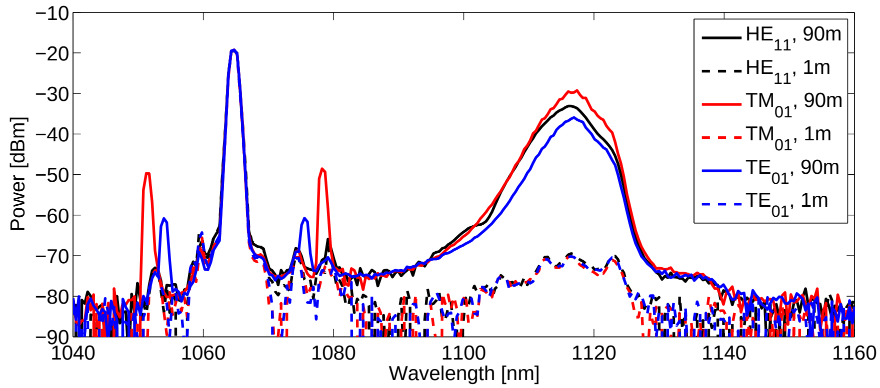

Fig. 3. Measured spectra after 90 m of propagation in the FMF.

a factor of two when both pump and signal are scalar modes [12]. A scalar mode is defined by having the same polarization direction at any point over the cross section of the mode; examples include modes described by the LP mode picture. It is noted that the strength of the Raman process also depends on the dopant profile of the fiber, since the concentration of germanium is known to increase Raman scattering [3, 13]. For this fiber the TM_{01} or TE_{01} mode have high intensity in the outer ring of the refractive index profile where the germanium concentration is especially high, see Fig. 1. Therefore, the strength of the Raman scattering increases for processes where one of the interacting modes are in either the TM_{01} or TE_{01} mode.

Experimentally, it was observed that as expected there was a strong polarization dependence of the gain when pumping in the fundamental mode. This was observed both when altering the launched polarization in the fiber by adjusting PC1 in the setup, see Fig. 2, and when the polarization was changed along the fiber by repositioning the FMF. In this context repositioning the fiber means to gently bend, rotate, and move the entire fiber bundle after the LPG. When pumping in the HOMs the polarization was changed only by repositioning the fiber, since using a polarization controller on the FMF would induce strong mode coupling. When pumping in the TM_{01} mode the gain changes by approximately 4.5 dB for different polarizations at a pump power of 307 W. However, when pumping in the TE_{01} mode the gain difference was approximately 12.6 dB for the same pump power. It is speculated that the additional polarization sensitive gain for the TE_{01} mode is due to stronger mode coupling along the fiber, since the TE_{01} mode is closer in effective index to the HE_{21} modes than the TM_{01} mode is. Hereby, partially resulting in a scalar mode, namely the LP_{11} mode, which introduces polarization dependent gain.

A close up of the region around the pump is shown in Fig. 4. The peaks occurring symmetrically around the pump when pumping in either TE_{01} or TM_{01} mode are caused by FWM processes. The peaks are not observed when pumping in the fundamental mode, and depending on which of the two HOMs is used as the pump, the peaks shift by approximately 3 nm. This indicates that the peaks are caused by a phase matched process, i.e. a narrow phase matched wavelength region. The inset shows the power of the stokes (S) and anti-stokes (AS) lines when the pump is in the TM_{01} mode as a function of pump peak power. It is seen that the power of the stokes and anti-stokes lines starts to decrease for pump peak power levels above 300 W. This pump power level coincides with the onset of the second and third order stimulated Raman scattering (SRS) processes, therefore these SRS processes may deplete the pump leading to a decrease in the power of the stokes lines. Another possibility is that power from the stokes and

#197744 - $15.00 USD Received 17 Sep 2013; revised 10 Oct 2013; accepted 11 Oct 2013; published 15 Nov 2013

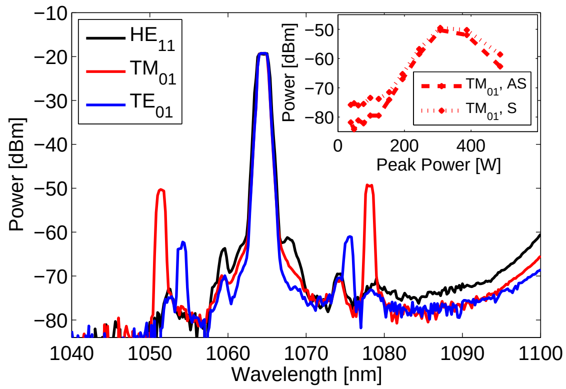

Fig. 4. Spectra after 90 m of propagation and 307 W of peak power, the pump mode is indicated by the legend. The OSA is saturated at the wavelength of the pump.

anti-stokes lines have started to couple back to the pump through the reverse FWM process [14].

At higher pump powers second order FWM lines were observed on either side of the pump. It was also observed that the FWM lines are polarization dependent, since the FWM lines are sensitive to repositioning of the FMF.

4. Mode images

To examine the modal content of different wavelengths regions of the spectra, seen in Fig. 3, filters were used and the modes were imaged using a CCD camera. Different sets of filters were used to filter out the two spectra shown in Fig. 5, for these spectra the pump was in the TE_{01} mode. For the blue line it is mainly the stokes line that remains, whereas for the green line it is only the first order Raman peak that remains. The spectral shape of the Raman peak is caused by the wavelength dependent transmission of the filters.

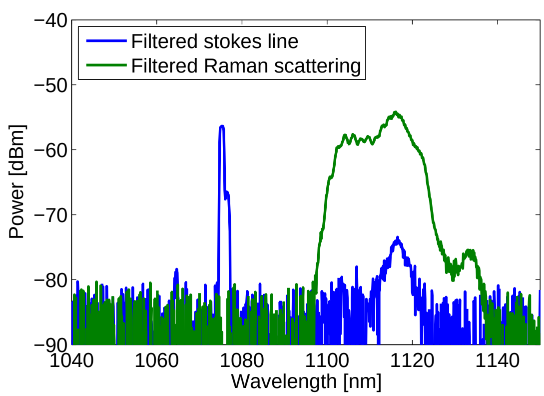

Fig. 5. Output spectra after 90 m of FMF with different combinations of bandpass and longpass filters.

Figure 6(a) shows the imaged mode of the Raman peak. It is seen that the light is in the fundamental mode in this wavelength region, since there is a dominant peak in the center surrounded by a ring of light with lower intensity in the outer ring of the refractive index profile.

#197744 - $15.00 USD Received 17 Sep 2013; revised 10 Oct 2013; accepted 11 Oct 2013; published 15 Nov 2013

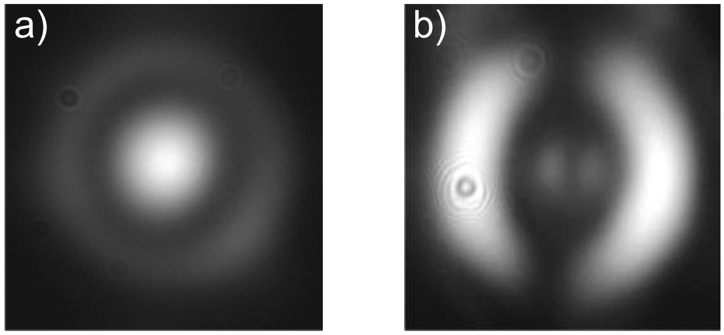

Fig. 6. The mode images for the two spectra shown in Fig. 5. a) The Raman peak. b) The FWM stokes line. The irregularity is due to a defect on the CCD chip of the camera.

Using a polarizer it was verified that the polarization of the mode is linear, hence there is no light in the TE_{01}, TM_{01} or HE_{21} modes at these wavelengths. Figure 6(b) shows the image of the FWM stokes peak, once again it was confirmed using a polarizer that the light is linearly polarized. Therefore, it appears that the light is in the LP_{12} mode. When the polarizer was oriented perpendicular to the LP_{12} mode, the remaining light showed a weak HE_{11} mode, which is assumed to be the residual light at the Raman peak, also observed in Fig. 5.

5. Conclusion

The Raman gain was measured between a pump at 1064 nm in either the HE_{11}, TE_{01}, or TM_{01} mode and a signal in the HE_{11} mode in a specialty designed fiber optimized for supporting full vectorial modes. It was verified by imaging that the signal remained in the fundamental mode in the FMF. Approximately 40 dB of Raman gain was obtained at 1117 nm in 90 m of FMF with a pump peak power of 307 W. Furthermore, when pumping in either the TE_{01} or TM_{01} mode a FWM process was observed at wavelengths close to the pump. By imaging and using filters and a polarizer it was shown that light at the stokes wavelength was in the LP_{12} mode.

Acknowledgment

The Danish Research Council for Technology and Production Sciences (project 09-066562) is acknowledged for financial support. OFS Fitel Denmark is acknowledged for providing the fiber.